Soils and Rocks
An International Journal of Geotechnical and Geoenvironmental Engineering
www.soilsandrocks.com
ISSN 1980-9743
ISSN-e 2675-5475

On the existence of a viscous component in the effective stress in clays

Ian Schumann Marques Martins[1], Vitor Nascimento Aguiar[2#], Paulo Eduardo Lima de Santa Maria[3], Rune Dyvik[4]

Article

Keywords
Effective stress
Viscous behavior
Consolidation
Stress relaxation
Time dependence

Abstract

This work explains secondary consolidation and undrained stress relaxation under isotropic (hydrostatic) stress states in saturated plastic soils, using an extended concept of effective stress. Effective stress (σ') is split into two components: one transmitted by the solid contacts between grains (σ'_s), called the solid component, and another transmitted by the highly viscous adsorbed water surrounding the grains (σ'_η), called the viscous component. Isotropic secondary consolidation is explained as taking place by the transference of the viscous component to the solid component under constant effective stress, suggesting that volume changes are associated to changes in the solid component and not to changes in effective stress as a whole. Isotropic consolidation tests in which drainage was closed after the "end of primary", starting an undrained isotropic stress relaxation stage, showed pore pressure increase with time under constant total stress, causing the effective stress to decrease with time, with no water content change. In the light of the extended concept of effective stress, such pore pressure build-up can be shown to be a consequence of the transference of the viscous component to pore pressure. A practical application of this approach is the prediction of the final value of volumetric strain caused by secondary consolidation. A model based on such an extended concept of effective stress is being developed for general stress states, being able to explain time and strain rate phenomena observed in plastic soil behavior, such as creep, shear stress relaxation and strain rate-dependent strength.

1. Introduction

Models for predicting soil behavior rely on the Principle of Effective Stress (PES), as introduced by Terzaghi (1936). However, there are some phenomena, especially in plastic soils, such as strain rate-dependent strength, creep, stress relaxation and secondary consolidation, which do not obey the PES (e.g., Martins, 1992; Chandler et al., 2004). In view of the theoretical difficulties when dealing with such phenomena, the usual approach is to preserve the essence of the PES and develop an additional tool to tackle the specific problem which is outside the framework of the PES. An example is the C_α/C_c = constant approach, proposed by Mesri & Godlewski (1977), to evaluate secondary consolidation (see Martins & Lacerda, 1989). In the authors' opinion, a better approach is the one taken by Terzaghi (1941) and Taylor (1942), who proposed to expand the original PES to explain secondary consolidation. In such a proposition, effective stress is split into two components: one that takes place through solid-to-solid contacts between grains, and the other that is carried by the highly viscous adsorbed water surrounding the soil grains. This paper shows that such a proposition can be used to explain not only isotropic secondary consolidation but also undrained isotropic stress relaxation, suggesting that both phenomena have the same physical origin.

Many models of clay behavior taking into account time and strain rate effects have been developed. Regarding one-dimensional consolidation, examples can be found in Taylor & Merchant (1940), Šuklje (1957), Gibson & Lo (1961), Barden (1965), Bjerrum (1967), Garlanger (1972), Martins & Lacerda (1985), Imai & Tang (1992), Yin & Graham (1996), Watabe & Leroueil (2015), among others. With the advance of computer-aided numerical analysis, more sophisticated stress-strain-strength models have been developed, such as Kutter & Sathialingam (1992), Tatsuoka et al. (2002), Yin et al. (2002), Qu et al. (2010), Bodas Freitas et al. (2011), Clarke & Hird (2012), Yin (2015), and Kurz et al. (2016). Nevertheless, except for Tatsuoka et al. (2002), none of them have considered Terzaghi's (1941) and Taylor's (1942) broad concept of effective stress.

#Corresponding author. E-mail address: vitoraguiar@poli.ufrj.br
[1]Universidade Federal do Rio de Janeiro, Instituto Alberto Luiz Coimbra de Pós-Graduação e Pesquisa de Engenharia, Programa de Engenharia Civil, Rio de Janeiro, RJ, Brasil.
[2]Universidade Federal do Rio de Janeiro, Escola Politécnica, Departamento de Construção Civil/Geotecnia, Rio de Janeiro, RJ, Brasil.
[3]SM Engenheiros Consultores Ltda, Rio de Janeiro, RJ, Brasil.
[4]Norges Geotekniske Institutt, Geoteknisk Laboratorium, Oslo, Norge.

Submitted on June 11, 2025; Final Acceptance on September 18, 2025; Discussion open until May 31, 2026.
Editor: Renato P. Cunha
https://doi.org/10.28927/SR.2026.009725

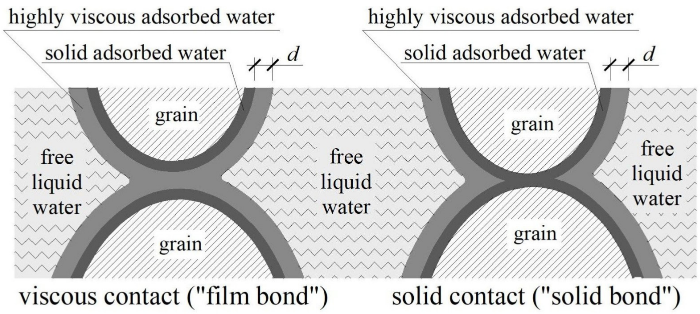

Figure 1. Types of inter-particle contacts (adapted from Terzaghi, 1941).

The aim of this paper is to investigate the validity of Terzaghi's (1941) and Taylor's (1942) proposition, showing experimental evidence of the existence of a viscous component of effective stress via isotropic consolidation/undrained stress relaxation tests. It includes results from an on-going laboratory test program to study clay rheology, initiated in the early 1980s.

2. Theoretical and experimental background

According to Terzaghi (1941), adsorbed water is in a solid state in the immediate vicinity of the surface of a clay particle and is strongly adhered to it (Figure 1). For the sake of simplicity, Terzaghi (1941) pictured clay particles with rounded shape. Beyond the thickness where adsorbed water is solid, the water is highly viscous, the viscosity decreasing with distance from the particle surface. For distances greater than a limit value "*d* ", viscous water becomes free water. The thickness "*d* " depends on the chemical properties of the solid particles and substances within the adsorption zone, e.g. sodium salts (Skempton & Northey, 1952; Bjerrum, 1954; Hvorslev, 1960; Lambe & Whitman, 1979, p. 20). Thus, in a clay, two types of inter-particle contact occur: "solid bonds" (herein called "solid contacts"), established through the solid adsorbed water, and "film bonds" (herein called "viscous contacts"), established through the highly viscous adsorbed water. Terzaghi (1941) stated that, as both types of contact transmit interparticle forces, the effective stress must be divided into two parts: (1) the "solid bond stress" (herein called "solid component of effective stress"), denoted by σ'_s, carried by the solid contacts, and (2) the "film bond stress" (herein called "viscous component of effective stress"), denoted by σ'_η, carried by the viscous contacts. Terzaghi (1941) explained secondary consolidation as the squeezing out of the viscous adsorbed water between grains in viscous contacts, which become solid contacts with time (see also Lambe & Whitman, 1979, p. 299).

Taylor (1948, pp. 243-247) used the above-mentioned concept to discuss the "plastic lag which occurs after the conclusion of primary compression" during one-dimensional consolidation. Vertical effective stress was assumed to be made up of two components: the "plastic resistance to compression", "dependent mainly on speed of compression", and the other ("the static case pressure"), dependent only on the void ratio. The latter would be associated with the one-dimensional compression curve corresponding to $\dot{\varepsilon}_v = 0$, a possibility that Graham et al. (1983), Leroueil et al. (1985) and Martins et al. (1997) test results suggested as a lower boundary for the set of strain rate dependent compression curves ε_v vs. σ'_v (*log*) or *e* vs. σ'_v (*log*) (Figure 2). A practical application of this approach is the prediction of the final value of settlement caused by secondary consolidation, a feature that the C_α / C_c approach (Mesri & Godlewski, 1977) does not provide. In the authors' opinion, the dependency of one-dimensional compression curves on $\dot{\varepsilon}_v$ is a manifestation of the viscous nature of clay behavior given by σ'_η.

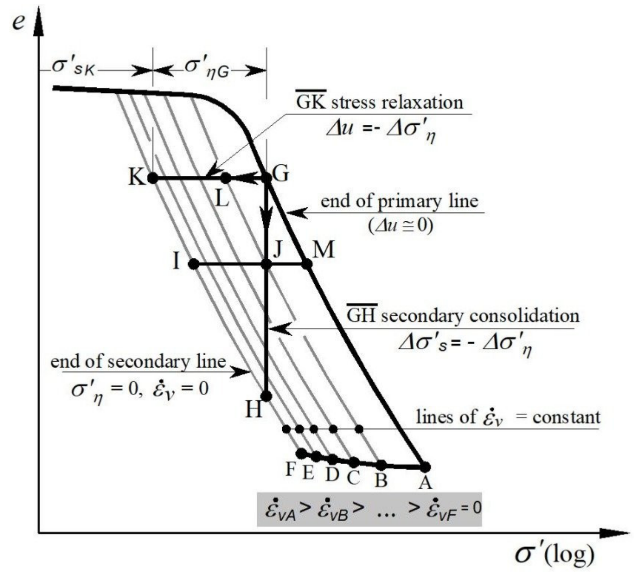

Figure 2. Isotropic secondary consolidation and undrained isotropic stress relaxation paths.

The aim of this paper is to show experimental evidence of the existence of the viscous component σ'_η in the effective stress. Although the approach can be extended to general stress states, the following analysis will be restricted to isotropic stress states for a clear understanding of the fundamental concepts.

It is assumed that, during isotropic consolidation of a clay specimen, effective stress σ' is made up of two components: a solid component σ'_s and a viscous component σ'_η . Hence, the equation of the PES becomes:

$$\sigma = \sigma'_s + \sigma'_\eta + u \tag{1}$$

with

$$\sigma'_s + \sigma'_\eta = \sigma' \tag{2}$$

Where σ is the applied isotropic total stress, σ' is the current value of the isotropic effective stress and u is the pore pressure.

To check whether Equation 1 holds true, isotropic consolidation tests were performed based on the following: For a given time during consolidation, in a given point of the specimen, since all planes are free from shear stresses, each variable in Equation 1 has the same magnitude in all planes. At the "end of primary" consolidation (point G in Figure 2), when the pore pressure u becomes negligible, since the applied total stress σ is held constant, the effective stress σ' must also be constant. Therefore, during secondary consolidation (GH line in Figure 2), volumetric strains keep occurring under constant ($\sigma'_s + \sigma'_\eta$). Hence, according to the Terzaghi's (1941) mechanism, secondary consolidation takes place by transferring σ'_η to σ'_s, with the viscous contacts becoming solid contacts over time. The "end of primary" line (Figure 2) can be viewed as the upper boundary line where the excess pore pressure is negligible and $\dot{\varepsilon}_v$ = constant. The path followed during secondary consolidation crosses isotache ($\dot{\varepsilon}_v$ = constant) lines parallel to the "end of primary" line, corresponding to decreasing $\dot{\varepsilon}_v$ (see Šuklje, 1957; Bjerrum, 1972). When all viscous contacts become solid contacts, secondary consolidation ends, with: $\dot{\varepsilon}_v = 0$, $\sigma'_\eta = 0$ and $\sigma = \sigma' = \sigma'_s$ (point H in Figure 2). The compression line for which $\dot{\varepsilon}_v = 0$ is called the "end of secondary" line.

It is worth saying that the term "secondary consolidation" is used herein just to refer to the period of the consolidation process which starts when the excess pore pressure becomes too small to be measured (i.e., negligible). The term "primary consolidation" is used to refer to the period from the beginning of the consolidation process until pore pressure becomes negligible. Obviously, the definition of how small pore pressure should be to be considered negligible is somewhat subjective. Nevertheless, although the article is focused on the "secondary consolidation" period, Equations 1 and 2 hold for the whole consolidation process, since the viscous phenomena (i.e., transference of σ'_η to σ'_s) is assumed to occur throughout the whole process, i.e. during both "primary" and "secondary" periods. This article is based on the assumption that clays behave according to hypothesis B (Jamiolkowski et al., 1985), following a unique stress-strain-strain rate relationship as proposed by Taylor (1942), Bjerrum (1972) and Leroueil et al. (1985).

According to the described mechanism, as secondary consolidation progresses along line GH (Figure 2), $\dot{\varepsilon}_v$ and σ'_η decrease towards $\dot{\varepsilon}_v = 0$ and $\sigma'_\eta = 0$ (see Taylor, 1948, p. 246). Therefore, σ'_η is associated to $\dot{\varepsilon}_v$ and, when $\dot{\varepsilon}_v = 0$, $\sigma'_\eta = 0$ (Point H).

In Figure 2, points K, I and H lie on the $\dot{\varepsilon}_v = 0$ compression line. As $\sigma'_\eta = 0$ on this line, the end of secondary line is the locus for which $\sigma' = \sigma'_s$, e.g., $\sigma'_K = \sigma'_{sK}$, $\sigma'_I = \sigma'_{sI}$ and $\sigma'_H = \sigma'_{sH}$. Thus, on the end of secondary line, σ'_s can be expressed as an exclusive function of void ratio e, i.e. $\sigma'_s = \sigma'_s(e)$. The smaller the void ratio, the higher the σ'_s value. Since σ'_η decreases during secondary consolidation and vanishes at the end of the process (point H), the current value of σ'_η corresponds to the horizontal distance from GH line and the end of secondary line (see Taylor, 1948, p. 245). Consequently, along a path following a fixed horizontal line (e = constant) there would be only changes in σ'_η, which means σ'_s = constant. This suggests that, for a fixed void ratio e, whatever the $\dot{\varepsilon}_v$ value, there is one and only one value of σ'_s and vice versa. From now on this will be used as a working hypothesis.

Considering points G and K (Figure 2), as both have the same void ratio, both are assumed to have the same σ'_s. Thus, σ' at point G (σ'_G) minus σ' at point K (σ'_K) corresponds to σ'_η at point G ($\sigma'_{\eta G}$). Similarly, σ' at point J (σ'_J) minus σ' at point I (σ'_I) corresponds to σ'_η at point J ($\sigma'_{\eta J}$) . This means that for every point to the right of the "end of secondary" line, σ'_η at a given point corresponds to the horizontal distance from the considered point to the "end of secondary" line (see Taylor, 1948, p. 245).

On the other hand, take the points L and J on the line $\dot{\varepsilon}_v = \dot{\varepsilon}_{vB}$ = constant (Figure 2). σ'_η at point L ($\sigma'_{\eta L}$) is:

$$\sigma'_{\eta L} = \sigma'_L - \sigma'_K \tag{3}$$

and σ'_η at point J ($\sigma'_{\eta J}$) is:

$$\sigma'_{\eta J} = \sigma'_J - \sigma'_I \tag{4}$$

Considering the $\dot{\varepsilon}_v$ = constant lines are parallel on the e vs. $\sigma'(log)$ plane:

$$\log\left(\sigma'_L\right) - \log\left(\sigma'_K\right) = \log\left(\sigma'_J\right) - \log\left(\sigma'_I\right) \tag{5}$$

$$\log\left(\frac{\sigma'_L}{\sigma'_K}\right) = \log\left(\frac{\sigma'_J}{\sigma'_I}\right) \tag{6}$$

$$\frac{\sigma'_L}{\sigma'_K} = \frac{\sigma'_J}{\sigma'_I} \tag{7}$$

Substituting the σ'_L and σ'_J values given by Equations 3 and 4 into Equation 7:

$$\frac{\sigma'_{\eta L} + \sigma'_K}{\sigma'_K} = \frac{\sigma'_{\eta J} + \sigma'_I}{\sigma'_I} \tag{8}$$

and then:

$$\frac{\sigma'_{\eta L}}{\sigma'_K} = \frac{\sigma'_{\eta J}}{\sigma'_I} \tag{9}$$

Combining Equations 7 and 9:

$$\frac{\sigma'_{\eta L}}{\sigma'_L} = \frac{\sigma'_{\eta J}}{\sigma'_J} \tag{10}$$

As $\sigma'_J > \sigma'_L$ (Figure 2), hence $\sigma'_{\eta J} > \sigma'_{\eta L}$. As points J and L rest on the same $\dot{\varepsilon}_v$ line and $\sigma'_{\eta J} > \sigma'_{\eta L}$, σ'_η cannot be an exclusive function of $\dot{\varepsilon}_v$, but is also a function of the void ratio. This also shows that, for a given $\dot{\varepsilon}_v$ = constant, the smaller the void ratio, the greater the σ'_η. Thus, $\sigma'_\eta = \sigma'_\eta\left(e, \dot{\varepsilon}_v\right)$ and $\sigma'_s = \sigma'_s\,(e)$, meaning that σ'_η and σ'_s are respectively functions of $\left(e, \dot{\varepsilon}_v\right)$ and (e). Hence, Equation 1 can be rewritten as:

$$\sigma = \sigma'_s\left(e\right) + \sigma'_\eta\left(e, \dot{\varepsilon}_v\right) + u \tag{11}$$

From this mechanism, one point should be brought to discussion regarding the Principle of Effective Stress stated by Terzaghi (1936): since, during secondary consolidation, volumetric strains keep occurring under constant σ', volume changes cannot be assigned to changes in effective stress as a whole. Considering σ'_η is being transferred to σ'_s, volumetric strains would be associated with changes of σ'_s and not with changes in effective stress as a whole.

On the other hand, what would be expected if drainage was closed at the "end of primary" (point G in Figure 2), keeping the applied isotropic total stress constant? This type of test, called herein undrained isotropic stress relaxation test, was carried out on different clays and described by various researchers such as Bjerrum et al. (1958), Walker (1969), Arulanandan et al. (1971), Holzer et al. (1973), Vaid & Campanella (1977). The main result observed in all tests, following the closure of drainage, was an increase in pore pressure over time, assigned to the arrest of secondary consolidation.

Two additional features were observed by Arulanandan et al. (1971) and Holzer et al. (1973) on such a type of test carried out on San Francisco Bay Mud samples: (1) the greater the isotropic consolidation stress, the higher the pore pressure that developed, and; (2) the longer the specimen was left under secondary consolidation before closing drainage, the lower the pore pressure that developed.

It was suggested that the pore pressure build-up was possibly caused by drainage of water from micropores into macropores (see De Jong & Verruijt, 1965), a possibility that Wang & Xu (2007) showed to be inadequate to explain secondary consolidation.

It is worth noting that undrained isotropic stress relaxation does not obey the original PES (Terzaghi, 1936) since, if the pore pressure increases under constant total stress, the effective stress must decrease. According to the interpretation of the original PES (see for example Atkinson & Bransby, 1978, pp. 21-25), this would cause the specimen to expand, which does not occur since the drainage is closed.

As far as secondary consolidation is concerned, according to the original PES, the specimen is not expected to compress under constant isotropic effective stress. Therefore, isotropic secondary consolidation is also outside the original PES framework.

Lastly, although isotropic secondary consolidation and undrained isotropic stress relaxation cannot be explained by the original PES (Terzaghi, 1936), they can be explained by Terzaghi's (1941) and Taylor's (1942) extended concept of effective stress, as will be discussed further.

3. Experimental program and discussions

3.1 Tests on laboratory-manufactured samples

Thomasi (2000) carried out two isotropic consolidation tests in triaxial apparatus on a laboratory-fabricated sample of kaolin (80%) and bentonite (20%), by weight. Water was added to the mixture to produce a sample with a water content (w) of twice its liquid limit. It was then consolidated in two CBR test cylinders to a vertical stress of 30 kPa. Characterization test results showed: w_L = 93%, w_P = 22% (I_P = 71%) and G_s = 2.62. The characteristics of the two 140 mm high and 70 mm diameter cylindrical specimens, trimmed from the consolidated samples, are shown in Table 1.

To impose a state of stress as close to isotropic as possible throughout the specimens, "free ends" were used following the techniques suggested by Rowe & Barden (1964). Only radial drainage was allowed to provide uniform consolidation along the specimen height. Two slotted filter paper drains were placed around the specimens in contact with the upper porous stone, which was separated from the top of the specimen by an acrylic disc inserted between them.

The specimens were enclosed in two rubber membranes. The excess pore pressure was measured in the center of the specimen bottom (an undrained boundary). Both specimens were subjected to a stage of back-pressure (u_b) application to 50 kPa, attaining *B*-coefficient values (Skempton, 1954) greater than 0.98. The specimens then underwent isotropic consolidation (see Table 2). The all-around consolidation stress (σ'_c) was set to three times the vertical effective stress of 30 kPa used for the one-dimensional consolidation during sample preparation in order to minimize stress-induced anisotropy (Wroth & Houlsby, 1985). Both tests were carried out under the temperature of 19 ± 1°C.

After the "end of primary" consolidation, drainage was closed and pore pressure was observed to increase over time (Figure 3). Such pore pressure increase is denoted by Δu_η. It is observed that the higher the volumetric strain rate ($\dot{\varepsilon}_v$) when drainage was closed, the higher the pore pressure that developed.

Such pore pressure build-up over time after drainage closure can be explained in light of Equation 11 as follows:

As the applied isotropic total stress σ is kept constant, taking derivatives with respect to time of both sides of Equation 11 gives:

$$\frac{d\sigma_s'}{dt} + \frac{d\sigma_\eta'}{dt} + \frac{du}{dt} = 0,$$
$$\text{thus}: \frac{d\sigma_s'}{dt} = -\left(\frac{d\sigma_\eta'}{dt} + \frac{du}{dt}\right) \tag{12}$$

As previously discussed, based on the mechanism proposed by Terzaghi (1941), during secondary (isotropic) consolidation, the volumetric strain must be associated with changes in the solid component of effective stress σ'_s and not with changes in effective stress as a whole. This is in agreement with Equation 12 since, during secondary consolidation, as $du / dt = 0$ then $d\sigma_s' / dt = -d\sigma_\eta' / dt$.

Since volumetric strains are associated with changes in σ'_s, the coefficient of volumetric compressibility must be defined in terms of σ'_s as $m_{vs} = d\varepsilon_v / d\sigma_s'$, thus $d\varepsilon_v / dt$ can be written as:

$$\frac{d\varepsilon_v}{dt} = \frac{d\varepsilon_v}{d\sigma_s'}\frac{d\sigma_s'}{dt} \text{ or } \frac{d\varepsilon_v}{dt} = m_{vs}\frac{d\sigma_s'}{dt},$$
$$\text{thus}: \frac{d\sigma_s'}{dt} = \frac{1}{m_{vs}}\frac{d\varepsilon_v}{dt} \tag{13}$$

Table 1. Initial characteristics of the specimens of 80% kaolin and 20% bentonite (Thomasi, 2000).

Test	w (%)	γ (kN/m³)	e	S_r (%)
T5	101	14.2	2.65	99.9
T6	106	14.0	2.78	99.9

Table 2. Data from tests on specimens of 80% kaolin and 20% bentonite (Thomasi, 2000).

Test	σ'_c (kPa)	Δt-c (min)	e_c	$\dot{\varepsilon}_v$ (10^{-8} s^{-1})	Δt-u (min)	Δu_η (kPa)
T5	90	4705	1.38	1.5	12628	14.1
T6	90	10391	1.39	0.3	14382	8.3

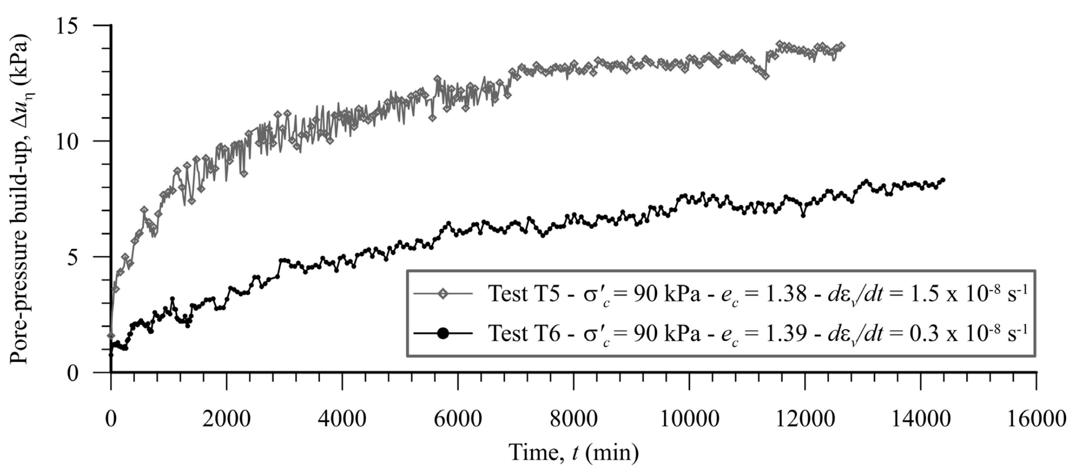

Figure 3. Pore pressure build-up after drainage closure on specimens of 80% kaolin and 20% bentonite (adapted from Thomasi, 2000).

Substituting $d\sigma_s^{'} / dt$ given by Equation 13 into Equation 12:

$$\frac{d\varepsilon_v}{dt} = -m_{vs}\left(\frac{d\sigma_\eta^{'}}{dt} + \frac{du}{dt}\right) \tag{14}$$

On the other hand, during undrained isotropic stress relaxation, as the soil is saturated and considering solid grains incompressible, water content is constant and volume changes can only be assigned to pore water volume changes due to pore water compressibility, no matter how small it is. Thus:

$$\frac{d\varepsilon_v}{dt} = \frac{d\varepsilon_v}{du}\frac{du}{dt} \tag{15}$$

Denoting the coefficient of compressibility of water by $m_w = d\varepsilon_{vw} / du$, ε_{vw} being the volumetric strain of water, the volumetric strain of a saturated soil with porosity n, under undrained conditions, is $\varepsilon_v = n\ \varepsilon_{vw}$. But the rate of change of ε_v with respect to pore pressure u can be taken as: $d\varepsilon_v / du \cong n\left(d\varepsilon_{vw} / du\right)$ (see Appendix 1), and therefore $d\varepsilon_v / du \cong n\,m_w$. Substituting this expression into Equation 15:

$$\frac{d\varepsilon_v}{dt} \cong n\,m_w\frac{du}{dt} \tag{16}$$

Substituting $d\varepsilon_v / dt$ given by Equation 16 into Equation 14:

$$\frac{du}{dt} \cong -\frac{1}{\underbrace{\left(1 + n\frac{m_w}{m_{vs}}\right)}_{B_s}}\frac{d\sigma_\eta^{'}}{dt} \tag{17}$$

The above derivation of coefficient B_s follows similar steps of the derivation of the Skempton's (1954) pore pressure coefficient B.

In soft clays, as m_w is much lower than m_{vs} and n is always smaller than 1, B_s can be taken as 1, hence:

$$\frac{du}{dt} \cong -\frac{d\sigma_\eta^{'}}{dt} \tag{18}$$

After closing drainage, pore pressure is experimentally observed to increase with time (see Figure 3). As a consequence, according to Equation 16, soil volume changes keep occurring due to the water compression caused by the pore pressure increase, with constant water content. However, although du / dt is measurable, since water compressibility m_w is extremely small, $d\varepsilon_v / dt$ is imperceptibly small and so is ε_v. That is the reason why, for practical purposes, saturated soil specimens are assumed to suffer no volume changes under undrained conditions.

During secondary consolidation, soil volume changes are due to water content reduction, whereas, after closing drainage (undrained stress relaxation), soil volume changes are due to water compression (with constant water content), being so small that can be considered negligible. After drainage closure, the rate of pore pressure build-up $\left(du / dt\right)$ is experimentally observed to decrease with time and is expected to approach a zero value (see Figure 3). Being so, according to Equation 16, at drainage closure, volumetric strain rate does not instantaneously drop to zero, but also decays gradually, approaching zero with time. Rearranging Equation 17:

$$\frac{d\sigma_\eta^{'}}{dt} + \frac{du}{dt} \cong -\frac{n\,m_w}{m_{vs}}\frac{du}{dt} \tag{19}$$

Substituting Equation 19 into Equation 12:

$$\frac{d\sigma_s^{'}}{dt} \cong \frac{n\,m_w}{m_{vs}}\frac{du}{dt} \tag{20}$$

Again, in soft clays, as m_w is much lower than m_{vs} and n is always smaller than 1, $n\ (m_w / m_{vs})$ is so small that it can be considered negligible. Therefore, during undrained isotropic stress relaxation, although $\left(du / dt\right)$ is measurable, $d\sigma_s^{'} / dt$ is negligible. As $d\varepsilon_v / dt$ is also negligible, as already demonstrated by Equation 16, both σ'_s and void ratio can be considered constant for practical purposes.

During undrained isotropic stress relaxation, as the total stress σ is kept constant and σ'_s can be assumed constant, according to Equation 11, the sum $\sigma'_\eta + u$ can also be assumed constant. According to Equation 18, during undrained isotropic stress relaxation, as pore pressure u increases, σ'_η decreases by the same magnitude. In the beginning of the undrained isotropic stress relaxation stage, excess pore pressure build-up due to the transference of σ'_η, denoted by Δu_η, is zero and, at the end of the stress relaxation stage, it must reach a value corresponding to the value of σ'_η at the instant of drainage closure, provided the stage lasts enough to make $\left(du / dt\right)$ equal to zero.

According to the described mechanism, secondary consolidation takes place by transferring σ'_η to σ'_s, during which volumetric strain rate ($\dot{\varepsilon}_v$) decreases over time. Thus, the longer the time between the "end of primary" consolidation and the drainage closure, the more secondary consolidation that has already taken place and the lower the values of σ'_η and $\dot{\varepsilon}_v$ at drainage closure (Figure 2). Hence, the later the drainage closure after primary consolidation, the lower the expected pore pressure build-up during an undrained isotropic stress relaxation stage (see path GJI in Figure 2). This can be observed by comparing the results of tests T5 and T6 (Figure 3 and Table 2). After the end of secondary consolidation, there would be no remaining σ'_η to be transferred to σ'_s. Therefore, no pore pressure build-up would be expected if drainage was closed after the end of secondary consolidation (point H in Figure 2).

3.2 Tests on undisturbed clay samples from Sarapuí II Test Site

Aguiar (2014) ran a test program on undisturbed soft clay samples from the Sarapuí II test site, a swampy area next to Guanabara Bay, on the left bank of Sarapuí River, about 7 km north of the Rio de Janeiro city limits (see Ortigão et al., 1983; Danziger et al., 2019). The soft clay deposit extends from the ground surface to depths varying from 6.5 m to 10 m. The water table coincides with the ground surface. Characterization test results throughout the clay layer are shown in Figure 4 (Jannuzzi et al., 2015).

Samples were taken between 3.0 m and 4.0 m depth from borings two meters apart. Characterization test results are shown in Table 3. All specimens were trimmed between the depths of 3.25 m and 3.66 m. Average values of water content (w), unit weight of soil (γ) and void ratio (e) obtained from 13 specimens are shown in Figure 4. Between 3.0 m and 4.0 m depth, Jannuzzi et al. (2015) estimated an effective overburden stress of 11 kPa and obtained a preconsolidation stress of 25 kPa from standard incremental loading oedometer tests and an average undrained shear strength of 11 kPa from field vane tests. The clay fraction consisted of 16% illite, 36% smectite and 48% kaolinite by weight. The activity was 1.6.

The samples were taken with brass tube samplers with wall thickness of 1.5 mm, inside diameter of 98.3 mm (without clearance) and net length of 650 mm.

CIU triaxial tests were carried out on 140 mm high and 70 mm diameter specimens. Saturation was accomplished by applying a backpressure at the top of the specimen in two stages of 25 kPa each, giving a final backpressure of 50 kPa. A B-coefficient value greater than 0.98 was measured on all

Table 3. Data of Sarapuí II clay deposit from 3.0 m to 4.0 m depth (from authors).

Grain size Distribution			Atterberg Limits			Specific Gravity
Clay (%)	Silt (%)	Sand (%)	w_L (%)	w_P (%)	I_P (%)	G_s
85	8	7	187	51	136	2.56

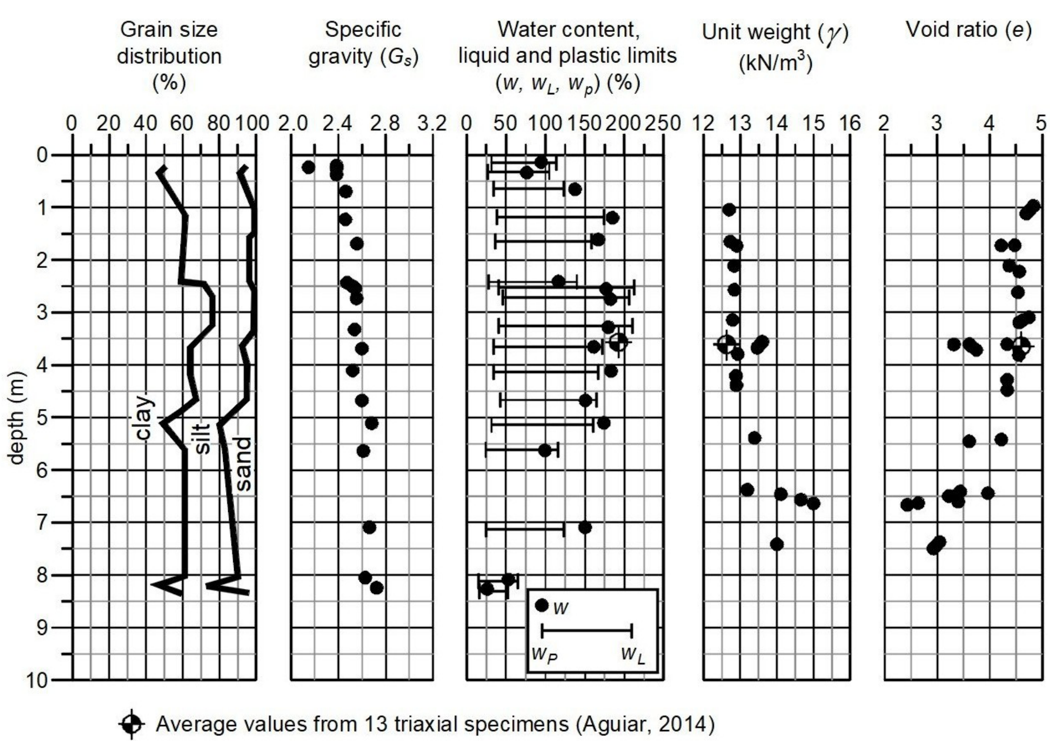

Figure 4. Geotechnical profile of Sarapuí II clay deposit (adapted from Jannuzzi et al., 2015).

specimens. During consolidation, drainage was provided through the top and the slotted filter paper placed around the specimen. Pore pressure was measured at the specimen bottom through a 10 mm diameter porous stone installed at the center of a 70 mm acrylic disk placed between the specimen bottom and the pedestal. A 70 mm diameter rubber membrane with a center hole slightly larger than 10 mm and lubricated with graphite powder on its lower surface was placed above the acrylic disk, providing a “free end”. The specimen was wrapped in one rubber membrane sealed to the pedestal and to the top cap. Silicone oil was used as cell fluid instead of water in order to minimize potential diffusion from the chamber into the specimen. All tests were carried out under the temperature of 19 ± 1°C.

Specimens were isotropically consolidated to 80, 140 and 200 kPa. The lowest value is higher than three times the preconsolidation stress so as to reduce structure and anisotropy effects.

In four tests (A1.1, A2.1, A3.1 and A6.1), drainage was closed when the excess pore pressure measured at the undrained boundary was less than 1% of the consolidation stress (σ'_c) and pore pressure was observed over time. The initial characteristics of these specimens are shown in Table 4 and test results are shown in Table 5 and Figure 5.

As observed by Arulanandan et al. (1971) and Thomasi (2000), pore pressure increased over time (see Figure 5), being greater for higher consolidation stresses. Such results along with Figure 2 suggest that, provided the volumetric strain rates ($\dot{\varepsilon}_v$) at the time of drainage closure are the same, during undrained isotropic stress relaxation, the pore pressure build-up plotted with time can be normalized respective to the consolidation stress, based on the following derivation (see Figure 2):

Table 4. Initial characteristics of the undisturbed Sarapuí II clay specimens (Aguiar, 2014).

Test	w	γ	e	S_r
	(%)	(kN/m³)		(%)
A1.1	171	12.7	4.38	100
A2.1	182	12.5	4.66	100
A3.1	185	12.5	4.74	100
A6.1	184	12.5	4.71	100

Table 5. Data from tests on undisturbed Sarapuí II clay specimens (Aguiar, 2014).

Test	σ'_c	Δt-c	e_c	$\dot{\varepsilon}_v$	Δt-u	Δu_η
	(kPa)	(min)		(10^{-7} s^{-1})	(min)	(kPa)
A1.1	80	1440	2.44	3.9	17316	23.6
A2.1	140	1440	2.20	2.6	17137	35.6
A3.1	200	2400	2.02	0.3	16163	46.3
A6.1	80	1440	2.62	3.1	29166	25.0

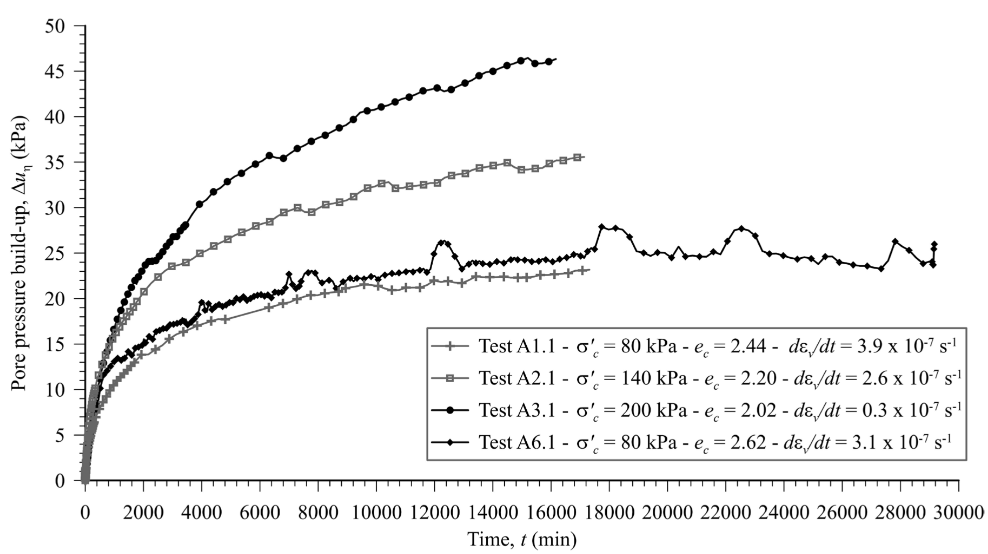

Figure 5. Pore pressure build-up after drainage closure on undisturbed Sarapuí II clay (Aguiar, 2014).

$$\log\left(\sigma'_G\right) - \log\left(\sigma'_L\right) = \log\left(\sigma'_M\right) - \log\left(\sigma'_J\right) \quad (21)$$

Thus:

$$\frac{\sigma'_G}{\sigma'_L} = \frac{\sigma'_M}{\sigma'_J} \quad (22)$$

Therefore:

$$\frac{\sigma'_G - \sigma'_L}{\sigma'_L} = \frac{\sigma'_M - \sigma'_J}{\sigma'_J} \quad (23)$$

and:

$$\frac{\sigma'_G - \sigma'_L}{\sigma'_G} = \frac{\sigma'_M - \sigma'_J}{\sigma'_M} \quad (24)$$

Where $(\sigma'_G - \sigma'_L)$ is the pore pressure build-up (Δu_η) developed between points G and L and $(\sigma'_M - \sigma'_J)$ is the pore pressure build-up (Δu_η) developed between points M and J. This derivation remains valid for any pair of paths from G and M on the same isotache line, provided they extend to corresponding points L and J on another isotache line. The remaining question is whether the time taken from G to L is the same as that from M to J. The results shown in Figure 6 seem to support this hypothesis (test A3.1 result is not included since its $\dot{\varepsilon}_v$ is about ten times smaller).

3.3 Tests on reconstituted Onsøy clay samples

A similar testing program consisting of ten triaxial tests was performed on reconstituted Onsøy clay samples at the Schmertmann Research Laboratory (Norwegian Geotechnical Institute, Oslo), at a temperature of 23 ± 1°C. The characterization and the engineering properties of the natural in situ Onsøy clay deposit were described by Lunne et al. (2003).

The 141 mm high and 72 mm diameter cylindrical specimens were trimmed from reconstituted Onsøy clay block samples: two prepared from the same slurry in 2016 by Suzuki et al. (2017) and a third one prepared from another slurry in 2017. A homogeneous slurry with water content of about twice the liquid limit was made by mixing amounts of disturbed Onsøy clay samples with deaired water with a salt content of 12 g/l, as in situ. The slurry was then consolidated in a large box in four stages up to a vertical effective stress (σ'_v) of 50 kPa in about four weeks (see Suzuki et al., 2017). Suzuki et al. (2017) obtained the following index properties for the material: G_s = 2.80, w_P = 29% and w_L = 68% (I_P = 39%).

The specimens, whose characteristics after trimming are shown in Table 6, were prepared and mounted according to NGI procedures (Berre, 1982; Lacasse & Berre, 1988). All specimens were wrapped in two rubber membranes. Silicone oil was used as cell fluid (except in tests SRL1.2 and SRL2.2, in which distilled water was used) to reduce possible diffusion from the cell fluid into the specimen.

Drainage was provided by porous stones on the top and bottom of the specimen and by four equally spaced filter paper strips placed in helical with a slope of 1V:1.3H along the specimen's lateral surface, from the top to the bottom porous stone. Specimen saturation was accomplished by applying a backpressure in three stages, two of 50 kPa and a final one of 100 kPa, giving a final backpressure of 200 kPa. A B-coefficient value higher than 0.98 was measured in all specimens. The specimens were then isotropically consolidated to the stresses indicated in Table 7.

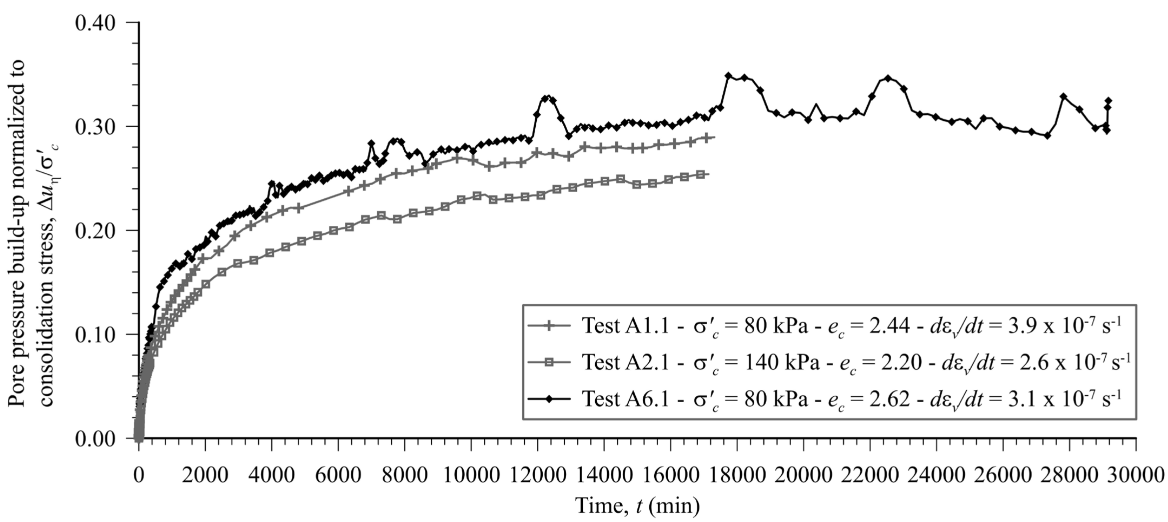

Figure 6. Normalized pore pressure build-up ($\Delta u_\eta/\sigma'_c$) after drainage closure on undisturbed Sarapuí II clay (Aguiar, 2014).

In all tests, drainage was closed after the end of primary (isotropic) consolidation and pore pressure measured over time. Drainage was closed when $\dot{\varepsilon}_v$ attained 10^{-7} s^{-1}, 10^{-8} s^{-1} or 10^{-9} s^{-1} (Table 7). Test results are shown in Table 7 and in Figures 7 to 12.

Figure 7 shows that, for a constant σ'_c, the greater the $\dot{\varepsilon}_v$ when drainage was closed, the greater the pore pressure build-up Δu_η. According to the mechanism already described, such pore pressure build-up is caused by the transference of σ'_η to pore pressure. As the higher the $\dot{\varepsilon}_v$ at the instant of drainage closure, the higher the σ'_η acting at that moment, thus higher Δu_η values are expected to develop after drainage closure. These results confirm why σ'_η must be written as a function of $\dot{\varepsilon}_v$ in Equation 11.

Figures 8 and 9 show that, for a fixed $\dot{\varepsilon}_v$ when drainage is closed, the greater the σ'_c, the greater the pore pressure build-up. For a given isotache ($\dot{\varepsilon}_v$= constant) line, as a higher σ'_c means a smaller void ratio, the smaller the void ratio at the instant of drainage closure (e_c), the higher the Δu_η developed, which means a higher σ'_η acting at drainage closure. These results confirm why σ'_η must also be written as a function of void ratio in Equation 11. Moreover, as observed in Sarapuí II clay, Figures 10 and 11 seem to support the hypothesis already discussed, namely: pore pressure build-up plotted with time can be normalized to the consolidation stress, provided the undrained isotropic stress relaxation stages start from points on the same isotache ($\dot{\varepsilon}_v$= constant) line.

If the undrained relaxation stress stages had lasted long enough, it would be expected that the value of Δu_η developed would become constant and correspond to the value of σ'_η acting at the moment of drainage closure. Moreover, according to Equation 9, for a fixed $\dot{\varepsilon}_v$ when drainage was closed, the value of σ'_η (and also the final Δu_η value) would be expected to normalize respective to the solid component of the consolidation stress (σ'_s). Unfortunately, this could not be checked due to the limited duration of the stress relaxation stages, even in Test 9.1, that lasted for more than 100 days (see Figure 12).

4. Discussion of the main points

The following aspects linking the experimental results to the theoretical background are highlighted below:

(a) Figures 3 and 7 show that, for a fixed σ'_c, the greater the $\dot{\varepsilon}_v$ at the beginning of an undrained isotropic stress relaxation stage (drainage closure), the greater the Δu_η value developed with time. This observation can be explained by the following reasoning.

Table 6. Initial characteristics of the reconstituted Onsøy clay specimens.

Test	w (%)	γ (kN/m^3)	e	S_r (%)
SRL1.2	57.1	16.3	1.65	97.0
SRL2.2	56.6	16.6	1.60	99.4
SRL3.1	59.3	16.3	1.68	98.7
SRL4.1	58.0	16.5	1.62	100
SRL4.2	57.8	16.5	1.62	99.6
SRL5.1	57.9	16.4	1.64	99.1
SRL5.2	57.5	16.5	1.63	99.1
SRL7.1	59.2	16.4	1.67	99.5
SRL7.2	58.8	16.4	1.66	99.2
SRL9.1	59.3	16.3	1.68	98.8

Table 7. Data from tests on reconstituted Onsøy clay specimens.

Test	σ'_c (kPa)	Δt-c (min)	e_c	$\dot{\varepsilon}_v$ (s^{-1})	Δt-u (min)	Δu_η (kPa)
SRL1.2	160	1580	1.33	0.9×10^{-7}	8919	40.9
SRL2.2	160	4500	1.29	1.0×10^{-8}	14809	29.1
SRL3.1	160	38604	1.30	0.9×10^{-9}	12839	15.7
SRL4.1	160	1454	1.31	0.7×10^{-7}	16432	35.0
SRL4.2	164	4800	1.30	1.1×10^{-8}	20100	31.1
SRL5.1	92.5	1440	1.44	1.1×10^{-7}	23394	24.9
SRL5.2	92.5	1380	1.42	1.1×10^{-7}	25920	28.4
SRL7.1	106	4860	1.40	0.6×10^{-8}	5190	12.4
SRL7.2	160	4620	1.31	0.7×10^{-8}	995	12.0
SRL9.1	160	37351	1.30	1.0×10^{-9}	141515	36.0

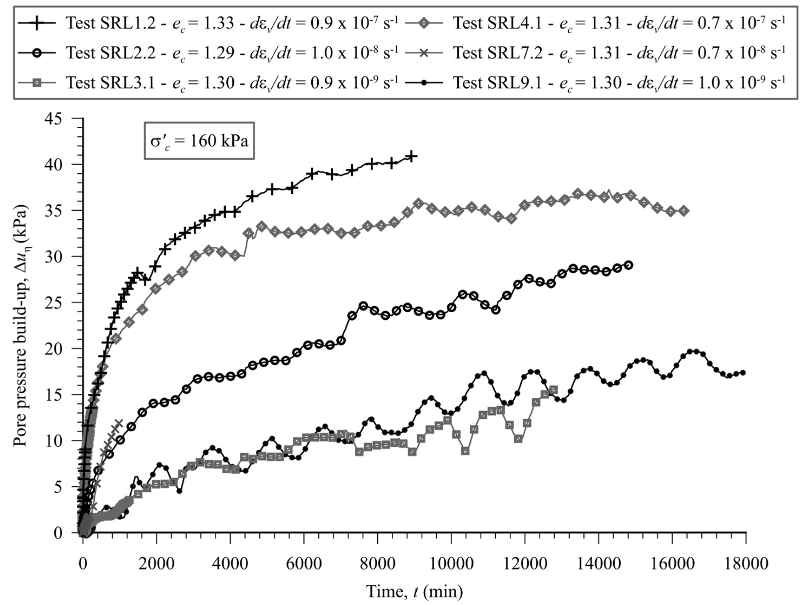

Figure 7. Pore pressure build-up after drainage closure after consolidation under σ'_c = 160 kPa on reconstituted Onsøy clay.

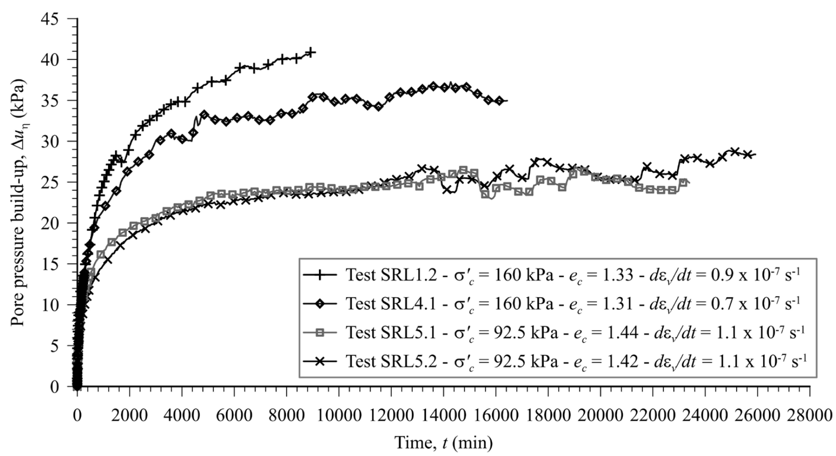

Figure 8. Pore pressure build-up after drainage closure with $\dot{\varepsilon}_v$ on the order of 10^{-7} s^{-1} on reconstituted Onsøy clay.

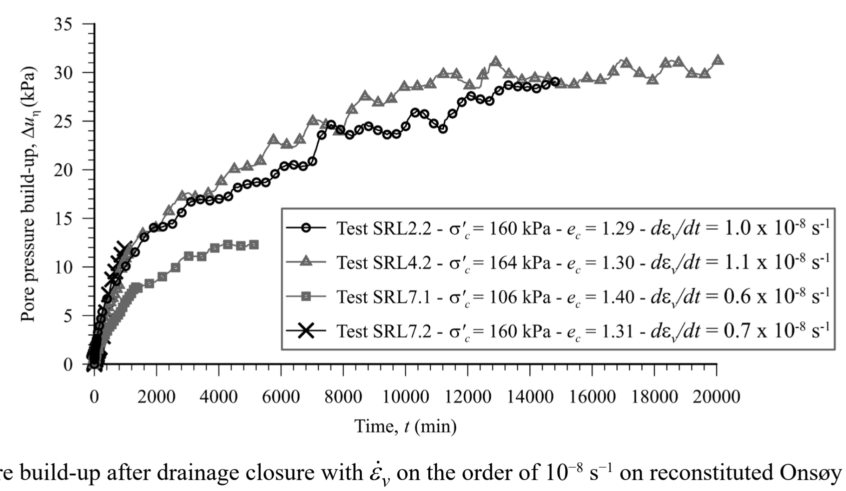

Figure 9. Pore pressure build-up after drainage closure with $\dot{\varepsilon}_v$ on the order of 10^{-8} s^{-1} on reconstituted Onsøy clay.

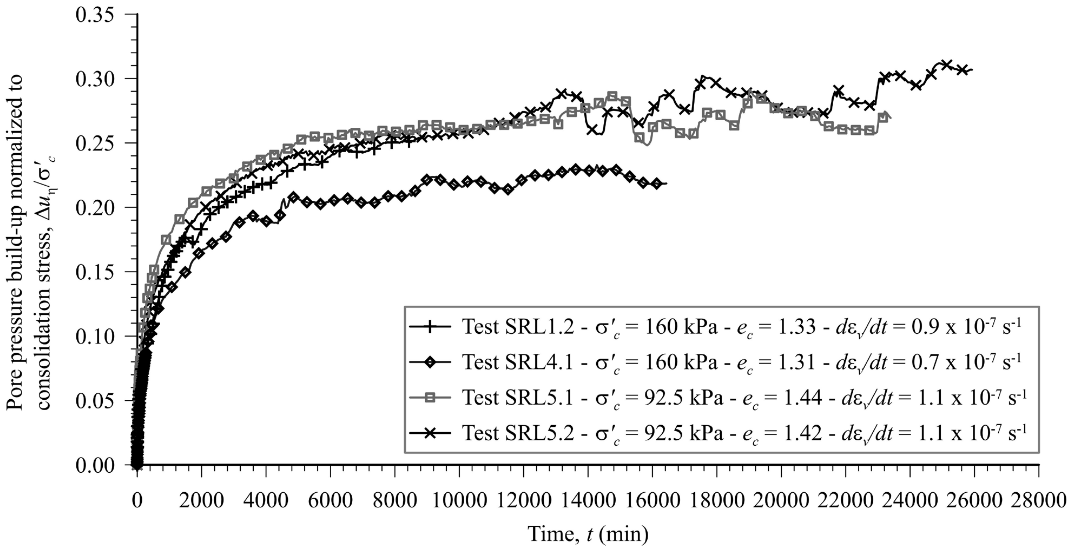

Figure 10. Normalized pore pressure build-up ($\Delta u_\eta/\sigma'_c$) after drainage closure with $\dot{\varepsilon}_v$ on the order of 10^{-7} s^{-1} on reconstituted Onsøy clay.

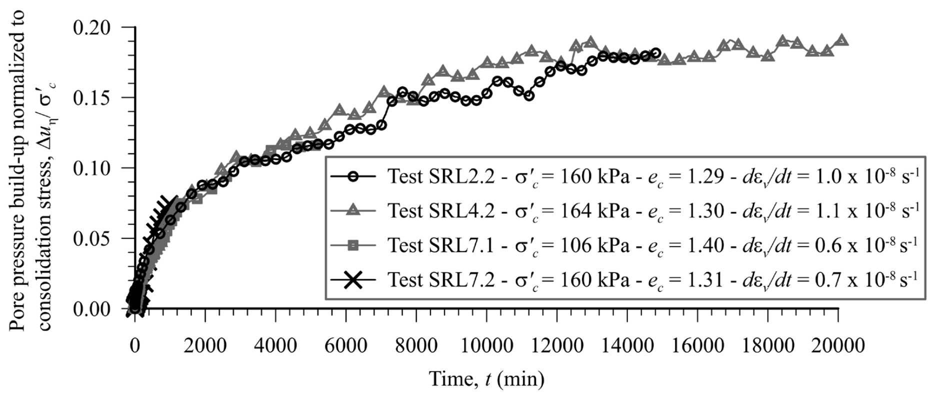

Figure 11. Normalized pore pressure build-up ($\Delta u_\eta/\sigma'_c$) after drainage closure with $\dot{\varepsilon}_v$ on the order of 10^{-8} s^{-1} on reconstituted Onsøy clay.

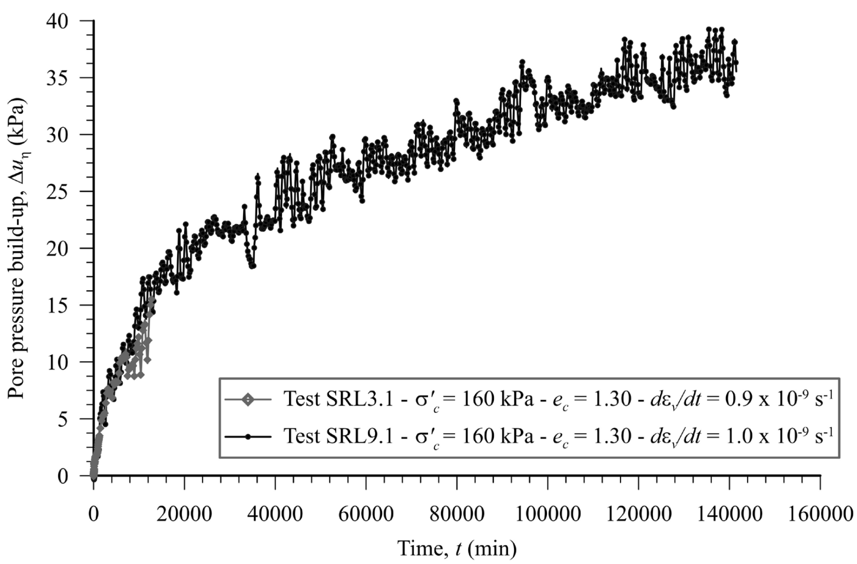

Figure 12. Pore pressure build-up after drainage closure with $\dot{\varepsilon}_v$ on the order of 10^{-9} s^{-1} on reconstituted Onsøy clay.

Consider first an undrained isotropic stress relaxation stage following GK line in Figure 2. Since the process is undrained with pore pressure generation, there must be pore water volume decrease (with constant water content). However, as the water compressibility is extremely small, path GK can be considered horizontal ($\varepsilon_v \cong 0$), as it is usually presumed in soil mechanics. At the beginning (point G), σ'_η is represented by the GK segment ($\sigma'_{\eta G}$). As stress relaxation progresses, according to Equation 18, an increase in pore pressure corresponds to an equal decrease in σ'_η. At the end of the process (point K), Δu_η generated must be equal to $\sigma'_{\eta G}$. Next consider an undrained isotropic stress relaxation stage following the JI segment in Figure 2. At the beginning (point J) σ'_η is represented by the JI segment ($\sigma'_{\eta J}$), which is smaller than GK segment ($\sigma'_{\eta J} < \sigma'_{\eta G}$). At the end of the process (point I), Δu_η generated must be equal to $\sigma'_{\eta J}$, and, therefore, smaller than the Δu_η generated at the end of GK stress relaxation. As σ'_c at point G and at point J are the same, but $\dot{\varepsilon}_v$ at point G is greater than $\dot{\varepsilon}_v$ at point J, this means that, for a fixed σ'_c, the greater the $\dot{\varepsilon}_v$ at the beginning of an undrained stress relaxation stage (drainage closure), the greater the expected Δu_η value at the end of the process. Although the tests were not long enough for fully stable Δu_η, this is the trend shown in Figures 3 and 7.

(b) Figures 5, 8 and 9 show that, for a given $\dot{\varepsilon}_v$, the greater the σ'_c at the beginning of an undrained isotropic stress relaxation stage (drainage closure), the greater the Δu_η value developed with time. Moreover, Figures 6, 10 and 11 suggest that Δu_η vs. t curves are proportional to σ'_c. This observation can be explained by the following reasoning. Consider two undrained isotropic stress relaxation stages starting from points on the same isotache line but different σ'_c, for instance points L and J on $\dot{\varepsilon}_{vB}$ line in Figure 2. Assuming parallel isotache lines, the Δu_η value expected at the end of both processes are proportional to σ'_s during the stress relaxation ($\sigma'_K = \sigma'_{sK}$ and $\sigma'_I = \sigma'_{sI}$ in Figure 2), as Equation 9 shows. However, according to Equation 10: $\sigma'_{\eta L}/\sigma'_L = \sigma'_{\eta J}/\sigma'_J$. This means that, for a fixed $\dot{\varepsilon}_v$, the greater the σ'_c at the beginning of an undrained isotropic stress relaxation stage (drainage closure), the greater the expected Δu_η value at the end of the process. Although the tests were not long enough, that is the trend shown in Figures 5, 8 and 9. Equation 10 also shows that the expected Δu_η value is directly proportional to σ'_c provided the starting points are on the same isotache line. In this case, the curves Δu_η vs. t can be normalized respective to σ'_c as suggested by Figures 6, 10 and 11.

(c) If it is assumed that the void ratio is constant during an undrained isotropic stress relaxation stage (GK segment in Figure 2), thus $\dot{\varepsilon}_v$ should be zero. If it was the case, as $\sigma'_\eta = f(e, \dot{\varepsilon}_v)$, σ'_η should not be expected to vary during stress relaxation. This apparent inconsistency can be cleared up by the following discussion. As pore pressure is observed to increase with time $(du/dt > 0)$, according to Equation 16, volumetric strain is not zero $(d\varepsilon_v/dt > 0)$, although water content is constant. However, as water compressibility (m_w) is extremely small and the porosity (n) is less than 1, the product $(n\, m_w\, du/dt)$ is negligible. As already demonstrated, $d\varepsilon_v/du \cong n\ m_w$. Therefore:

$$\int_0^{\varepsilon_v(t)} d\varepsilon_v \cong \int_0^{\Delta u_\eta(t)} n\, m_w\, du \tag{25}$$

Assuming n and m_w changes are of secondary order when compared to pore pressure changes, both n and m_w can be assumed constant, thus:

$$\int_0^{\varepsilon_v(t)} d\varepsilon_v \cong n\, m_w \int_0^{\Delta u_\eta(t)} du \tag{26}$$

and

$$\varepsilon_v(t) \cong n\, m_w\ \Delta u_\eta(t) \tag{27}$$

For example: For test SRL 9.1 shown in Figure 12, since the void ratio (e_c) is 1.30, the porosity (n) is 0.57. For the time corresponding to the end of the test, Δu_η was 36.0 kPa (see Table 7 and Figure 12). Taking the compressibility of pure water (m_w) (without dissolved gas) equal to 5×10^{-7} kPa^{-1}, thus, at that time:

$$\varepsilon_v \cong 0.57 \cdot 5\ \text{x}10^{-7} \cdot 36 = 1.03\ \text{x}10^{-5} = 1.03\ \text{x}10^{-3}\ \% \tag{28}$$

Therefore:

$$\Delta e = 1.03\ \text{x}10^{-5} \cdot (1 + 1.3) = 2.36\ \text{x}10^{-5}\ . \tag{29}$$

These values of ε_v and Δe are negligible.

(d) The experimental results show that, during undrained isotropic stress relaxation, under constant total stress, the pore pressure increases making the effective stress to decrease with negligible volume change (zero volume change for all practical purposes).

(e) Considering isotropic secondary consolidation (GH line in Figure 2), during which σ'_c is constant and σ'_η is assumed to be transferred to σ'_s, the smaller the $\dot{\varepsilon}_v$, the smaller the σ'_η. The magnitude of σ'_η corresponds to the horizontal distance between the

(e, σ'_c) point and the end of secondary line. At point G, where $\dot{\varepsilon}_v = \dot{\varepsilon}_{vA}$ (Figure 2), σ'_η, denoted by $\sigma'_{\eta G}$, is represented by the GK segment. At point J, where $\dot{\varepsilon}_v = \dot{\varepsilon}_{vB}$, σ'_η, denoted by $\sigma'_{\eta J}$, is represented by the JI segment. When secondary consolidation reaches point H, σ'_η is zero and secondary consolidation ends. According to Equation 12, since, during isotropic secondary consolidation, $du / dt = 0$, thus $d\sigma'_s / dt = -d\sigma'_\eta / dt$. This shows that secondary consolidation takes place by transferring σ'_η to σ'_s, being in accordance to Terzaghi's (1941) proposition. Moreover, it shows that, during isotropic secondary consolidation, volumetric strains should be assigned to changes in the solid component of effective stress (σ'_s), which increases during the process, and not to changes in the effective stress as a whole, which is kept constant.

5. Conclusion

a) When dealing with soil mechanics phenomena which do not obey the original Principle of Effective Stress (PES), the usual approach is to develop a special tool to tackle the specific problem. In this paper, a broader concept of effective stress introduced by Terzaghi (1941) and Taylor (1942) is used to explain secondary consolidation and undrained stress relaxation under isotropic stress states in saturated plastic soils.

b) In this approach, the effective stress is split into two components: a solid component (σ'_s), transmitted by the solid contacts between grains, and a viscous component (σ'_η), transmitted by the highly viscous adsorbed water surrounding the grains. Theoretical reasoning supported by experimental evidence shows that σ'_s is an exclusive function of void ratio (e), whereas σ'_η, is a function of volumetric strain rate ($\dot{\varepsilon}_v$) and void ratio (e).

c) In the light of this approach, isotropic secondary consolidation takes place under constant effective stress (σ') by transferring σ'_η to σ'_s. Thus, volumetric strains should be associated with changes in σ'_s, which increases during the process, and not with changes in effective stress as a whole (σ'), which remains constant.

d) If drainage is closed after the "end of primary" isotropic consolidation, starting an undrained isotropic stress relaxation, pore pressure is observed to increase with time. As total stress is kept constant, effective stress decreases with negligible volume decrease (with constant water content) due to the extremely low compressibility of the water, showing again that volumetric strains cannot be associated to changes in effective stress as a whole. According to this approach, such pore pressure build-up can be explained by the transference of σ'_η to pore pressure, with constant σ'_s.

e) Conclusions (c) and (d) combined suggest that, under isotropic stress states, whenever there is change in σ'_s, there must be change in void ratio, and conversely.

f) Undrained isotropic stress relaxation tests carried out on three different clays by closing the drainage after the "end of primary" isotropic consolidation showed the following features: (i) For a fixed value of consolidation stress (σ'_c), the greater the volumetric strain rate ($\dot{\varepsilon}_v$) at drainage closure, the higher the pore pressure Δu_η that developed. (ii) For a fixed $\dot{\varepsilon}_v$ at drainage closure, the greater the σ'_c value (i.e. the smaller the void ratio), the greater the pore pressure (Δu_η) that developed. In case (ii), Δu_η (t) seems to normalize respective to $\sigma'_{c.}$

g) During undrained isotropic stress relaxation, a pore pressure increase corresponds to a σ'_η decrease of the same magnitude (Equation 18). As a consequence and to provide the balance of Equation 11, pore pressure (Δu_η) must rise with time towards the value of σ'_η existing at drainage closure. On the other hand, at the end of secondary consolidation, $\sigma'_\eta = 0$. Therefore, if drainage was closed after the end of secondary consolidation, no pore pressure build-up would be expected, since there would be no σ'_η to be transferred to pore pressure.

h) The proposed mechanism, based on Terzaghi (1941) and Taylor (1942), does not invalidate the Principle of Effective Stress, but extends it to explain isotropic secondary consolidation and undrained isotropic stress relaxation in saturated plastic soils within a unique framework. The authors have been working to extend this approach to general stress states.

Acknowledgements

The authors would like to thank Prof. Fernando Danziger and Prof. Graziella Jannuzzi for their help in taking the Sarapuí II clay samples, Diego Silva for his help to the second author in carrying out the triaxial tests on Sarapuí II clay, Yusuke Suzuki, Toralv Berre, James Olaka as well as others NGI colleagues for their help with NGI triaxial test procedures and Prof. John Schmertmann for discussions about Sarapuí II clay and reconstituted Onsøy clay test results. The authors also thanks Dr. José Luiz Clemente for having made valuable comments that made the article more readable.

The authors also thank Coordenação de Aperfeiçoamento de Pessoal de Nível Superior (Capes) for sponsoring the doctoral program of Vitor Aguiar at Coppe/UFRJ, Fundação de Amparo à Pesquisa do Estado do Rio de Janeiro (Faperj) for sponsoring his post-doctoral program at Coppe/UFRJ, Research Council of Norway and Norwegian Geotechnical Institute (NGI) for sponsoring his post-doctoral program at NGI and for the use of the laboratory facilities in the Schmertmann Research Laboratory (SRL).

Declaration of interest

The authors have no conflicts of interest to declare. All co-authors have observed and affirmed the contents of the paper and there is no financial interest to report.

Authors' contributions

Ian Schumann Marques Martins: conceptualization, data curation, formal analysis, funding acquisition, investigation, methodology, project administration, resources, supervision, validation, visualization, writing - original draft, writing - review and editing. Vitor Nascimento Aguiar: conceptualization, data curation, formal analysis, investigation, validation, visualization, writing - original draft, writing - review and editing. Paulo Eduardo Lima de Santa Maria: conceptualization, methodology, writing - review and editing. Rune Dyvik: conceptualization, funding acquisition, resources, supervision, writing - review and editing.

Data availability

All data produced or examined in the course of the current study are included in this article.

Declaration of use of generative artificial intelligence

This work was prepared without the assistance of any generative artificial intelligence (GenAI) tools or services. All aspects of the manuscript were developed solely by the authors, who take full responsibility for the content of this publication.

List of symbols and abbreviations

d	Distance from clay grain surface beyond which adsorbed water turns into free water
e	Void ratio
e_c	Void ratio when drainage was closed (after primary consolidation)
m_{vs}	Coefficient of volumetric compressibility of soil related to σ'_s
m_w	Coefficient of volumetric compressibility of water
n	Porosity
t	Time
u	Pore pressure
u_b	Back-pressure
w	Water content
w_L	Liquid limit
w_P	Plastic limit
B_s	Pore pressure coefficient similar to Skempton's pore pressure coefficient B
Capes	Coordenação de Aperfeiçoamento de Pessoal de Nível Superior
Coppe	Instituto Alberto Luiz Coimbra de Pós-graduação e Pesquisa de Engenharia
C_c	Compression index
C_α	Rate of secondary consolidation
Faperj	Fundação Carlos Chagas Filho de Amparo à Pesquisa do Estado do Rio de Janeiro
G_s	Specific gravity
I_P	Plasticity index
NGI	Norwegian Geotechnical Institute
PES	Principle of Effective Stress
S_r	Degree of saturation
SRL	Schmertmann Research Laboratory
UFRJ	Universidade Federal do Rio de Janeiro
V	Total volume of soil
V_v	Volume of soil voids
V_w	Volume of water that fills the soil voids
Δt-c	Time during which consolidation was allowed
Δt-u	Time during which drainage valve was kept closed after consolidation
Δu	Excess pore pressure
Δu_η	Pore pressure build-up due to the transference of σ'_η to pore pressure
ε_v	Soil volumetric strain
ε_{vw}	Water volumetric strain
$\dot{\varepsilon}_v$	Soil volumetric strain rate (equal to $d\varepsilon_v/dt$)
γ	Unit weight of soil
σ	Normal total stress / isotropic total stress
σ'	Normal effective stress / isotropic effective stress / current value of isotropic effective stress
σ'_c	Consolidation stress
σ'_s	Solid component of normal (isotropic) effective stress
σ'_v	Vertical effective stress
σ'_η	Viscous component of normal (isotropic) effective stress

References

Aguiar, V.N. (2014). *Contribuição ao estudo das relações tensão-deformação-resistência-tempo das argilas moles* [Doctoral thesis, Federal University of Rio de Janeiro (Coppe/UFRJ)]. Federal University of Rio de Janeiro's repository (in Portuguese). Retrieved in June 11, 2025, from http://www.coc.ufrj.br/pt/teses-de-doutorado/381-2014/8105-vitor-nascimento-aguiar

Arulanandan, K., Shen, C.K., & Young, R.B. (1971). Undrained creep behaviour of a coastal organic silty clay. *Geotechnique*, *21*(4), 359-375. https://doi.org/10.1680/geot.1971.21.4.359.

Atkinson, J.H., & Bransby, P.L. (1978). *The mechanics of soils: an introduction to critical state soil mechanics*. McGraw-Hill.

Barden, L. (1965). Consolidation of clay with non-linear viscosity. *Geotechnique*, *15*(4), 345-362. https://doi.org/10.1680/geot.1965.15.4.345.

Berre, T. (1982). Triaxial testing at the Norwegian Geotechnical Institute. *Geotechnical Testing Journal*, *5*(1-2), 3-17. https://doi.org/10.1520/GTJ10794J.

Bjerrum, L. (1954). Geotechnical properties of Norwegian marine clays. *Geotechnique*, *4*(2), 49-69. https://doi.org/10.1680/geot.1954.4.2.49.

Bjerrum, L. (1967). Engineering geology of Norwegian normally-consolidated marine clays as related to settlements of buildings. *Geotechnique*, *17*(2), 83-118. https://doi.org/10.1680/geot.1967.17.2.83.

Bjerrum, L. (1972). Embankments on soft ground: state-of-the-art report. In American Society of Civil Engineers (Eds.), *Proceedings of the Specialty Conference on Performance of Earth- Supported Structures: June 11-14, 1972 Purdue University, Lafayette, Indiana: Jointly Sponsored by School of Civil Engineering, Purdue University and Soil Mechanics and Foundations Division ASCE* (Vol. 2, pp. 1-54). Reston: ASCE.

Bjerrum, L., Simons, N., & Torblaa, I. (1958). The effect of time on the shear strength of a soft marine clay. In Groupement Belge de la Société Internationale de Mécanique des Sols et des Travaux de Fondations (Eds.), *Brussels Conference 58 on Earth Pressure Problems* (Vol. 1, pp. 148-158). Brussels: International Society of Soil Mechanics and Foundation Engineering.

Bodas Freitas, T.M., Potts, D.M., & Zdravkovic, L. (2011). A time dependent constitutive model for soils with isotach viscosity. *Computers and Geotechnics*, *38*(6), 809-820. https://doi.org/10.1016/j.compgeo.2011.05.008.

Chandler, R.J., Freitas, M.H., & Marinos, P. (2004). Geotechnical characterization of soils and rocks: a geological perspective. *Advances in Geotechnical Engineering: The Skempton Conference*, 67-102.

Clarke, S.D., & Hird, C.C. (2012). Modelling of viscous effects in natural clays. *Canadian Geotechnical Journal*, *49*(2), 129-140. https://doi.org/10.1139/t11-084.

Danziger, F.A.B., Jannuzzi, G.M.F., & Martins, I.S.M. (2019). The relationship between sea-level change, soil formation and stress history of a very soft clay deposit. *AIMS Geosciences*, *5*(3), 461-479. https://doi.org/10.3934/geosci.2019.3.461.

DeJong, G.J., & Verruijt, A. (1965). Primary and secondary consolidation of a spherical clay sample. In International Society for Soil Mechanics and Geotechnical Engineering (Eds.), *Proceedings of the 6th International Conference on Soil Mechanics and Foundation Engineering* (Vol. 1, pp. 254-258). Toronto: University of Toronto Press.

Garlanger, J.E. (1972). The consolidation of soils exhibiting creep under constant effective stress. *Geotechnique*, *22*(1), 71-78. https://doi.org/10.1680/geot.1972.22.1.71.

Gibson, R.E., & Lo, K.Y. (1961). A theory of consolidation for soils exhibiting secondary compression. *Norwergian Geotechnical Institute Publication*, *41*, 1-16.

Graham, J., Crooks, J.H.A., & Bell, A.L. (1983). Time effects on the stress-strain behaviour of natural soft clays. *Geotechnique*, *33*(3), 327-340. https://doi.org/10.1680/geot.1983.33.3.327.

Holzer, T.L., Höeg, K., & Arulanandan, K. (1973). Excess pore pressures during undrained clay creep. *Canadian Geotechnical Journal*, *10*(1), 12-24. https://doi.org/10.1139/t73-002.

Hvorslev, M.J. (1960). Physical components of the shear strength of saturated clays. In American Society of Civil Engineers (Eds.), *Proceedings of the ASCE Research Conference on Shear Strength of Cohesive Soils* (pp. 169-273). New York: ASCE.

Imai, G., & Tang, Y.-X. (1992). A constitutive equation of one-dimensional consolidation derived from inter-connected tests. *Soil and Foundation*, *32*(2), 83-96. https://doi.org/10.3208/sandf1972.32.2_83.

Jamiolkowski, M., Ladd, C.C., Germaine, J.T., & Lancellota, R. (1985). New developments in field and laboratory testing of soils. In International Society for Soil Mechanics and Geotechnical Engineering (Eds.), *Proceedings of the 11th International Conference on Soil Mechanics and Foundation Engineering* (Vol. 1, pp. 57-153). Rotterdam: A.A. Balkema Publishers.

Jannuzzi, G.M.F., Danziger, F.A.B., & Martins, I.S.M. (2015). Geological-geotechnical characterisation of Sarapuí II clay. *Engineering Geology*, *190*, 77-86. https://doi.org/10.1016/j.enggeo.2015.03.001.

Kurz, D., Sharma, J., Alfaro, M., & Graham, J. (2016). Semi-empirical elastic-thermoviscoplastic model for clay. *Canadian Geotechnical Journal*, *53*(10), 1583-1599. https://doi.org/10.1139/cgj-2015-0598.

Kutter, B.L., & Sathialingam, N. (1992). Elastic-viscoplastic modelling of the rate-dependent behaviour of clays. *Geotechnique*, *42*(3), 427-441. https://doi.org/10.1680/geot.1992.42.3.427.

Lacasse, S., & Berre, T. (1988). Triaxial testing methods for soils. *Advanced Triaxial Testing of Soil and Rock*, 977, 264-289.

Lambe, T.W., & Whitman, R.V. (1979). *Soil mechanics, SI Version*. John Wiley & Sons.

Leroueil, S., Kabbaj, M., Tavenas, F., & Bouchard, R. (1985). Stress-strain-strain rate relation for the compressibility of sensitive natural clays. *Geotechnique*, *35*(2), 159-180. https://doi.org/10.1680/geot.1985.35.2.159.

Lunne, T., Long, M., & Forsberg, C.F. (2003). Characterization and engineering properties of Onsøy clay. In T.S. Tan (Eds.), *Characterization and engineering properties of natural soils* (Vol. 1, pp. 395-427). Balkema.

Martins, I.S.M. (1992). *Fundamentos de um modelo de comportamento de solos argilosos saturados* [Doctoral thesis, Federal University of Rio de Janeiro (Coppe/UFRJ)]. Federal University of Rio de Janeiro's repository (in Portuguese). Retrieved in June 11, 2025, from http://www.coc.ufrj.br/pt/teses-de-doutorado/136-1992/769-ian-schumann-marques-martins

Martins, I.S.M., & Lacerda, W.A. (1985). A theory of consolidation with secondary compression. In International Society for Soil Mechanics and Geotechnical Engineering (Eds.), *Proceedings of the 11th International Conference on Soil Mechanics and Foundation Engineering* (Vol. 2, pp. 567-570). Toronto: University of Toronto Press.

Martins, I.S.M., & Lacerda, W.A. (1989). Discussion of "C_α/C_c *concept and* K_0 *during secondary compression*" by G. Mesri and A. Castro. *Journal of Geotechnical Engineering*, *115*(2), 264-267. https://doi.org/10.1061/(ASCE)0733-9410(1989)115:2(264).

Martins, I.S.M., Santa Maria, P.E.L., & Lacerda, W.A. (1997). A brief review about the most significant results of COPPE research on rheological behaviour of saturated clays subjected to one-dimensional strain. In M. Almeida (Ed.), *Recent developments in soil and pavement mechanics* (pp. 255-264). Balkema.

Mesri, G., & Godlewski, P.M. (1977). Time and stress-compressibility interrelationship. *Journal of Geotechnical Engineering*, *103*(GT5), 417-430. http://dx.doi.org/10.1061/AJGEB6.000042.

Ortigão, J.A.R., Werneck, M.L.G., & Lacerda, W.A. (1983). Embankment failure on clay near Rio de Janeiro. *Journal of Geotechnical Engineering*, *109*(11), 1460-1479. https://doi.org/10.1061/(ASCE)0733-9410(1983)109:11(1460).

Qu, G., Hinchberger, S.D., & Lo, K.Y. (2010). Evaluation of the viscous behaviour of clay using generalized overstress viscoplastic theory. *Geotechnique*, *60*(10), 777-789. https://doi.org/10.1680/geot.8.P.031.

Rowe, P.W., & Barden, L. (1964). Importance of free ends in triaxial testing. *Journal of the Soil Mechanics and Foundations Division*, *90*(SM1), 1-27. https://doi.org/10.1061/JSFEAQ.0000586.

Skempton, A.W. (1954). The pore pressure coefficients A and B. *Geotechnique*, *4*(4), 143-147. https://doi.org/10.1680/geot.1954.4.4.143.

Skempton, A.W., & Northey, R.D. (1952). The sensitivity of clays. *Geotechnique*, *3*(1), 30-53. https://doi.org/10.1680/geot.1952.3.1.30.

Šuklje, L. (1957). The analysis of the consolidation process by isotaches method. In International Society for Soil Mechanics and Geotechnical Engineering (Eds.), *Proceedings of the 4th International Conference on Soil Mechanics and Foundation Engineering* (Vol. 1, pp. 200-206). London: Butterworths Publications Ltd.

Suzuki, Y., Dyvik, R., & Schmertmann, J.H. (2017). Experimental study on use internal and external drains in triaxial tests. *Geotechnical Testing Journal*, *40*(5), 810-821. https://doi.org/10.1520/GTJ20160266.

Tatsuoka, F., Ishihara, M., Di Benedetto, H., & Kuwano, R. (2002). Time-dependent shear deformation characteristics of geomaterials and their simulation. *Soil and Foundation*, *42*(2), 103-129. https://doi.org/10.3208/sandf.42.2_103.

Taylor, D.W. (1942). *Research on consolidation of clays*. Cambridge: Massachusetts Institute of Technology.

Taylor, D.W. (1948). *Fundamentals of Soil Mechanics*. John Wiley & Sons. https://doi.org/10.1097/00010694-194808000-00008.

Taylor, D.W., & Merchant, W. (1940). A theory of clay consolidation accounting for secondary compression. *Journal of Mathematics and Physics*, *19*(3), 167-185. https://doi.org/10.1002/sapm1940191167.

Terzaghi, K. (1936). The shearing resistance of saturated soils and the angle between the planes of shear. In International Society for Soil Mechanics and Geotechnical Engineering (Eds.), *Proceedings of the 1st International Conference on Soil Mechanics and Foundation Engineering* (2nd ed., Vol. 1, pp. 54-56). Cambridge: Harvard University.

Terzaghi, K. (1941). Undisturbed clay samples and undisturbed clay. *Journal of the Boston Society of Civil Engineers*, *28*(3), 45-65.

Thomasi, L. (2000). *Sobre a existência de uma parcela viscosa na tensão normal efetiva* [Master's dissertation, Federal University of Rio de Janeiro (Coppe/UFRJ)]. Federal University of Rio de Janeiro's repository (in Portuguese). Retrieved in June 11, 2025, from http://www.coc.ufrj.br/pt/dissertacoes-de-mestrado/100-2000/1723-luciana-thomasi

Vaid, Y.P., & Campanella, R.G. (1977). Time-dependent behaviour of undisturbed clay. *Journal of the Geotechnical Engineering Division*, *103*(GT7), 693-709. https://doi.org/10.1061/AJGEB6.0000449.

Walker, L.K. (1969). Undrained creep in a sensitive clay. *Geotechnique*, *19*(4), 515-529. https://doi.org/10.1680/geot.1969.19.4.515.

Wang, Y.H., & Xu, D. (2007). Dual porosity and secondary consolidation. *Journal of Geotechnical and Geoenvironmental Engineering*, *133*(7), 793-801. https://doi.org/10.1061/(ASCE)1090-0241(2007)133:7(793).

Watabe, Y., & Leroueil, S. (2015). Modelling and implementation of the isotache concept for long-term consolidation behavior. *International Journal of Geomechanics*, *15*(5), 1-8. https://doi.org/10.1061/(ASCE)GM.1943-5622.0000270.

Wroth, C.P., & Houlsby, G.T. (1985). Soil Mechanics - Property characterization and analysis procedures. In International Society for Soil Mechanics and Geotechnical Engineering (Eds.), *Proceedings of the 11th International Conference on Soil Mechanics and Foundation Engineering* (Vol. 1, pp. 1-55). Toronto: University of Toronto Press.

Yin, J.-H., & Graham, J. (1996). Elastic visco-plastic modelling of one-dimensional consolidation. *Geotechnique*, *46*(3), 515-527. https://doi.org/10.1680/geot.1996.46.3.515.

Yin, J.-H., Zhu, J.-G., & Graham, J. (2002). A new elastic viscoplastic model for time-dependent behaviour of normally and overconsolidated clays: theory and verification. *Canadian Geotechnical Journal*, *39*(1), 157-173. https://doi.org/10.1139/t01-074.

Yin, J.-H. (2015). Fundamental issues of elastic viscoplastic modeling of the time-dependent stress-strain behavior of geomaterials. *International Journal of Geomechanics*, *15*(5), A4015002. https://doi.org/10.1061/(ASCE)GM.1943-5622.0000485.

Appendix 1. Derivation of $d\varepsilon_v / du \cong n\, d\varepsilon_{vw} / du$.

This appendix shows the derivation of $d\varepsilon_v / du \cong n\, d\varepsilon_{vw} / du$, where ε_v is the soil volumetric strain, n is the soil porosity and ε_{vw} is the water volumetric strain.
Firstly, it is worth recalling that, for a saturated soil: $\varepsilon_v = n\, \varepsilon_{vw}$. Therefore:

$$\frac{d\varepsilon_v}{du} = \frac{d\left(n\,\varepsilon_{vw}\right)}{du} = \varepsilon_{vw}\frac{dn}{du} + n\frac{d\varepsilon_{vw}}{du} \tag{30}$$

Being saturated soil, $V_v = V_w$, where V_v is the volume of voids and V_w is the volume of water that fills the voids. Hence, the porosity n is $n = V_w / V$, where V is the total volume of soil. Thus:

$$\varepsilon_{vw}\frac{dn}{du} = \varepsilon_{vw}\frac{d\left(V_w / V\right)}{du} = \varepsilon_{vw}\left(\frac{1}{V}\frac{dV_w}{du} - \frac{V_w}{V^2}\frac{dV}{du}\right) \tag{31}$$

And, therefore, Equation 31 can be rewritten as:

$$\varepsilon_{vw}\frac{dn}{du} = \varepsilon_{vw}\left(\frac{n}{V_w}\frac{dV_w}{du} - \frac{n}{V}\frac{dV}{du}\right) \tag{32}$$

As $d\varepsilon_v = dV / V$ and $d\varepsilon_{vw} = dV_w / V_w$, hence Equation 32 is rewritten as:

$$\varepsilon_{vw}\frac{dn}{du} = \varepsilon_{vw}\left(n\frac{d\varepsilon_{vw}}{du} - n\frac{d\varepsilon_v}{du}\right) \tag{33}$$

Substituting Equation 33 into Equation 30:

$$\frac{d\varepsilon_v}{du} = \varepsilon_{vw}\left(n\frac{d\varepsilon_{vw}}{du} - n\frac{d\varepsilon_v}{du}\right) + n\frac{d\varepsilon_{vw}}{du} \tag{34}$$

Rearranging Equation 34:

$$\frac{d\varepsilon_v}{du} = n\frac{d\varepsilon_{vw}}{du}\frac{\left(1+\varepsilon_{vw}\right)}{\left(1+n\,\varepsilon_{vw}\right)} \tag{35}$$

As ε_{vw} is extremely small when compared to 1 and $n < 1$:

$$\frac{\left(1+\varepsilon_{vw}\right)}{\left(1+n\,\varepsilon_{vw}\right)} \cong 1 \tag{36}$$

And finally:

$$\frac{d\varepsilon_v}{du} \cong n\frac{d\varepsilon_{vw}}{du} \tag{37}$$